HHS Public Access

Author manuscript

Oncogene. Author manuscript; available in PMC 2011 July 06.

Published in final edited form as:

Oncogene. 2011 January 6; 30(1): 32–42. doi:10.1038/onc.2010.389.

Direct interaction between NHERF1 and Frizzled regulates β-catenin signaling

David S. Wheeler[1,2], **Stacey R. Barrick**[1], **Melanie J. Grubisha**[1,2], **Adam M. Brufsky**[3,4], **Peter A. Friedman**[1,3], and **Guillermo Romero**[1,4]

[1]Laboratory of GPCR Biology, Department of Pharmacology and Chemical Biology, University of Pittsburgh School of Medicine, Pittsburgh, PA 15261, USA.

[2]Medical Scientist Training Program, University of Pittsburgh School of Medicine, Pittsburgh, PA 15261, USA.

[3]Department of Medicine, University of Pittsburgh School of Medicine, Pittsburgh, PA 15261, USA.

[4]University of Pittsburgh Cancer Institute, University of Pittsburgh School of Medicine, Pittsburgh, PA 15261, USA.

Abstract

While Wnt-Frizzled (Fzd) signaling is critical in the pathophysiology of carcinomas, its role in human breast cancer has been difficult to establish. We show here that the adaptor protein Na^+/H^+ Exchange Regulatory Factor1 (NHERF1), a protein abundantly expressed in normal mammary epithelium, regulates Wnt signaling, maintaining low levels of β-catenin activation. NHERF1's effects are mediated by direct interactions between one of its PSD-95/Drosophila discs large/ZO-1 domains (PDZ domains) and the C-terminus of a subset of Fzd receptors. Loss of NHERF1 in breast cancer cell lines enhances canonical Wnt signaling and Wnt-dependent cell proliferation. Furthermore, the mammary glands of NHERF1 knockout mice exhibit increased mammary duct density accompanied by increased proliferation and β-catenin activity. Finally, we demonstrate a negative correlation between NHERF1 expression and nuclear β-catenin in human breast carcinomas. Taken together, these results provide novel insight into the regulation of Wnt signaling in normal and neoplastic breast tissues, and identify NHERF1 as an important regulator of the pathogenesis of breast tumors.

Aberrant Wnt signaling causes breast neoplasia in animal models (reviewed in (Fantozzi & Christofori, 2006)). In humans, however, the involvement of Wnt signaling in breast cancer pathogenesis remains unclear. Stable, ectopic expression of specific Wnts can transform primary human mammary epithelium, which can form invasive tumors in mouse xenograft

---

AUTHOR CONTRIBUTIONS

D.S.W. and G.R. conceived the study, designed and executed experiments, analyzed the data and prepared the manuscript. S.R.B. aided with animal studies and designed experiments. M.J.G. performed biochemical assays. A.B. selected the human subjects and aided with pathological characterization. P.A.F. and G.R. supervised the analysis of the data and edited the manuscript.

Additional methods are listed in Supplementary materials.

models (Ayyanan et al., 2006). About 60% of breast cancers show evidence of increased β-catenin activity but the mechanism and significance of these observations have not been elucidated (Lin et al., 2000; Ryo et al., 2001).

The Na^+/H^+ exchange regulatory factor1 (NHERF1, also known as the Ezrin Binding Phosphoprotein of 50kDa, EBP50) is a cytosolic PDZ adaptor protein abundantly expressed in human mammary epithelium. NHERF1 was initially identified as a regulator of the localization, signaling and traffic of GPCRs, ion channels and transporters (reviewed in (Weinman et al., 2006)). Recently, NHERF1 has been proposed to function as a tumor suppressor (Dai et al., 2004; Kreimann et al., 2007; Pan et al., 2006). Knockdown of NHERF1 increases cellular proliferation and migration of various breast cancer cell lines (Pan et al., 2006; Pan et al., 2008). Furthermore, when introduced in a mouse xenograft model, NHERF1 knockout cells were more aggressive and produced greater numbers of metastases (Pan et al., 2006). NHERF1 mutations occur in 3% of human breast tumors while loss of heterozygosity (LoH) at the NHERF1 locus (17q25.1) occur in over 50% of primary beast tumors (Dai et al., 2004). Both are correlated with poor prognosis and early death (Dai et al., 2004).

The mechanism by which NHERF1 regulates tumor growth and migration is unclear. The search for potential NHERF1 targets revealed that 8 out of the 10 human Frizzled (Fzd) receptors terminate in a canonical PDZ ligand (x-S/T-x-V/L; see Figure 1a) (Songyang et al., 1997). Here, we investigated the hypothesis that NHERF1 directly interacts with Fzd receptors and regulates Wnt signaling. We show that NHERF1 interacts directly with a subset of Fzd receptors, and that ablation of NHERF1 increases Wnt signaling and Wnt-dependent proliferation. Furthermore, NHERF1 knockout mice exhibit enhanced β-catenin activation and increased mammary duct density. Finally, NHERF1 expression and β-catenin activation are negatively correlated in human breast tumors. Therefore, we conclude that NHERF1's function as a tumor suppressor is a consequence of its role in the regulation of canonical Wnt signaling.

RESULTS

NHERF1 binds Fzd receptors

We developed a Chinese Hamster Ovary cell model system (CHO-N10) in which NHERF1 expression is undetectable under basal conditions and induced by the addition of tetracycline (Wheeler et al., 2007). These cells express low levels of endogenous Fzd receptors (Supplementary Table 1). To investigate the interaction between NHERF1 and Fzd, CHO-N10 cells were transfected with HA-tagged human Fzd4 and induced by tetracycline to express NHERF1. As seen in Figure 1b, NHERF1 co-immunoprecipitated with Fzd4. To demonstrate that the interaction between Fzd4 and NHERF1 is governed by PDZ domain-PDZ ligand interactions, the C-terminal valine of Fzd4 was mutated to alanine (Fzd4 V537A). We previously showed that the equivalent mutation abrogates the interactions of NHERF1 with the parathyroid hormone receptor type 1 (PTH1R) (Wheeler et al., 2007). The interaction between the Fzd4 V537A and NHERF1 was reduced by 95% when compared to the wild type (Figure 1b, lanes 2 and 4). Therefore, NHERF1 binds Fzd4 via the receptor's terminal PDZ ligand.

To determine which of the two PDZ domains of NHERF1 was responsible for these interactions, we transfected CHO cells with NHERF1 variants in which the cores of PDZ1, PDZ2 and both PDZ1+PDZ2 had been mutated: S1 (defective PDZ1), S2 (defective PDZ2) and S1S2 (defective PDZ1 and PDZ2) (Wheeler et al., 2007). The data shown in Figure 1c demonstrate that the S1 mutant binds Fzd4 as effectively as wild-type NHERF1, whereas Fzd4 binding to the S2 and S1S2 variants is very significantly reduced. We conclude, therefore, that Fzd4 interacts preferentially with PDZ2.

Finally, to demonstrate that the interactions of Fzd4 and NHERF1 are direct, we performed an overlay assay using recombinant His-tagged NHERF1 purified from *E. coli*. The results, shown in Figure 1d, demonstrate that recombinant NHERF1 binds Fzd4, supporting the hypothesis that the interactions between NHERF1 and Fzd receptors are direct. Further support to the conclusion that these interactions are direct is the demonstration that the interaction of recombinant NHERF1 with V537A-Fzd4 is very significantly reduced when compared to the wild type receptor (Figure 1d).

Prior work demonstrated that NHERF1 tethers membrane proteins to the actin cytoskeleton localizing them to distinct stress fiber domains and decreasing their lateral mobility (Bates et al., 2006; Wheeler et al., 2007). NHERF1 expression caused Fzd4 to aggregate along phalloidin positive fibers in stark contrast to the uniform distribution observed in control cells (Figure 2a, 2b). The distribution of Fzd4 V537A was diffuse independently of NHERF1 expression (Figure 2c, 2d). Expression of S1-NHERF1 caused induced the redistribution of Fzd4 into bundle-like structures indistinguishable from those formed by expression of wild-type NHERF1 (Supplementary Figure 1a). As expected, this redistribution was not observed upon expression of the S2 or S1S2 NHERF1 constructs (Supplementary Fig 1b, 1c). When the lateral mobility of Fzd4-eGFP was measured using fluorescence recover after photobleaching (FRAP), NHERF1 expression decreased the diffusion coefficient of Fzd4-eGFP by 54% and increased the immobile fraction by over 5 fold (Figure 2e, 2f). These results demonstrate that the interaction of PDZ2 of NHERF1 with the terminal PDZ ligand of Fzd4 tether the receptor to the actin cytoskeleton.

Direct interaction with NHERF1 regulates Wnt signaling

To determine the effects of NHERF1 on Fzd signaling, Fzds 2, 3, 4, and 7 were transfected into CHO-N10 cells and β-catenin activation was measured using the TOP/FOP luciferase reporter assay. Based on their terminal amino acid sequence, Fzds 2, 4 and 7 are predicted to interact with NHERF1, while Fzd3 is not (Figure 1a). Wnt3a-conditioned medium induced β-catenin activation in cells expressing Fzd 2, 3 and 7 while Wnt5a-conditioned medium stimulated β-catenin activity in Fzd4-transfected cells. Fzds 2, 4 and 7 showed impaired Wnt-induced β-catenin activation in the presence of NHERF1 (76%, 86% and 74% decrease, respectively) (Figure 3a). In contrast, Wnt signaling via Fzd3 was unaffected by NHERF1 expression (Figure 3a). Likewise, the Fzd4 V537A was significantly less sensitive to NHERF1-induced inhibition, consistent with its inability to bind NHERF1 (Figure 3b).

We next examined the effects of the S1, S2 and S1S2 NHERF1 mutants on Wnt-induced β-catenin activation. S1-NHERF1 functioned identically to wild type while NHERF1 containing mutations in the second PDZ domain (S2 and S1S2) showed no inhibition of Wnt

signaling (Figure 3c). Thus, interaction between the second PDZ domain of NHERF1 and Fzd govern NHERF1-mediated regulation of Wnt signaling. Importantly, 2 of the 3 mutations detected in human breast cancer (K172N and R180W) are located within the second PDZ domain of NHERF1 (Dai et al., 2004).

Loss of NHERF1 expression in breast cancer cells enhances Wnt-induced β-catenin activation and cell proliferation

Since NHERF1 regulates Wnt signaling in CHO-N10 cells, we hypothesized that the tumor suppressor activity of NHERF1 in breast cancer may result from modulation of Wnt signaling. To investigate this, MCF7 and MDA MB-231 human breast cancer cell lines were selected because they have similar Fzd repertoires (Supplementary Table 1), while representing two extremes of NHERF1 expression. MCF7 cells express high levels of NHERF1 whereas MDA MB-231 cells express trace amounts (Figure 3d, Supplementary Figure 2a, Supplementary Table 1). Transient transfection with shRNA targeted against NHERF1 decreased protein expression by 95% in MCF7 cells (Figure 3d). Transfection of MDA MB-231 cells with NHERF1 was able to reconstitute NHERF1 expression to levels comparable to those observed in MCF-7 cells (Supplementary Figure 2a).

At baseline, both MCF7 and MDA MB-231 cells showed little β-catenin activation, suggesting that Wnt secretion and autocrine stimulation are not active. MCF7 cells showed no significant increase in β-catenin activation when stimulated with either Wnt3a- or Wnt5a-conditioned medium. In contrast, NHERF1 knockdown MCF7 cells responded to both Wnt3a and Wnt5a stimulation with approximately four fold increases in β-catenin activity (Figure 3e).

Cyclin-D1 is a well established target gene of β-catenin known to influence cellular proliferation and breast cancer prognosis (Gillett et al., 1996; Tetsu & McCormick, 1999; Umekita et al., 2002). Cyclin-D1 levels were evaluated by qPCR in control and NHERF1 knockdown MCF7 cells following treatment with Wnt5a. As expected, NHERF1 knockdown cells expressed significantly greater amounts of cyclin-D1 in response to Wnt (Figure 3f). Furthermore, both Wnt 3a and Wnt5a significantly increased the rate of proliferation NHERF1 knockdown MCF7 cells compared to control cells (Figure 3g).

This trend was recapitulated in the MDA MB-231 cells. Stimulation of control MDA MB-231 cells (lacking NHERF1) resulted in a significant activation of β-catenin. These effects were blocked by transfection with NHERF1 (Supplementary Figure 2).

Increased duct density and β-catenin levels in the mammary glands of NHERF1 knockout mice

Our *in vitro* data predict that the loss of NHERF1 in mammary tissue should result in increased Wnt signaling and a hyperproliferative phenotype. We examined the fourth and fifth mammary glands from 10 week old virgin NHERF1−/− mice and compared them to those of wild type littermates. Breast tissue from the NHERF1−/− mice exhibited greater density of mammary ducts (Figure 4a, 4b). A subset of the knockout mice (30–40%) manifested a more severe phenotype consisting of adipose atrophy accompanied by capillary

and ductal dilation (Figure 4c). Overall, loss of NHERF1 expression resulted in a three to four fold increase in duct density (Figure 4d). Because the total body weight and fat contents of NHERF1−/− mice were comparable to those of wild type animals, the observed increase in duct density is most likely the result of increased breast proliferation. This was confirmed using an *in vivo* BrdU staining protocol to identify proliferating cells in the mammary ducts. The results show increased incorporation of BrdU in the knock out mammary ducts (Figure 4e; $p<0.03$, $n=4$).

Mammary ducts from wild type animals showed strong NHERF1 staining along the apical membrane of epithelial cells and faint β-catenin staining along all epithelial membranes (Figure 4f). Ducts from NHERF1−/− animals had increased levels of β-catenin staining and a greater percentage of β-catenin localized within the nucleus (Figure 4f, 4g). Taken together these results suggest that loss of NHERF1 leads to increased ductal proliferation and density, which correlate with enhanced β-catenin activation.

Correlation between NHERF1 expression and β-catenin activation in human breast cancer tissues

β-catenin activation is a negative predictor of prognosis and survival in human breast cancer (Dolled-Filhart et al., 2006; Lin et al., 2000). Because our data link loss of NHERF1 expression to increased Wnt signal transduction, we predicted a negative correlation between NHERF1 expression and β-catenin activity in human tumor samples. To test this hypothesis, breast cancer biopsies of varying stages and ER/PR status were stained for NHERF1 and β-catenin (see Supplementary Table 2 for detailed characteristics of the clinical samples). Antibody staining demonstrated low levels of β-catenin in tumors expressing high levels of NHERF1, independently of their ER/PR status. Furthermore, β-catenin staining was weak and membrane delimited in high-NHERF1 tumors, resembling the pattern observed in mammary tissues from wild type mice (Figure 5a). In contrast, β-catenin expression was greater in tumors that expressed little or no NHERF1 (Figure 5b). This increased expression was accompanied by an increase in the percent of β-catenin observed within the nucleus. Furthermore, the aggregated data demonstrated a strong negative correlation between NHERF1 expression and the fraction of β-catenin within the nucleus ($r=0.69$, $F=8.729$, $p = .0105$) (Figure 5c). Further analysis demonstrated this negative correlation to be independent of ER/PR status and tumor stage. In normal control tissues, nuclear β-catenin staining was uniformly low and unrelated to NHERF1 staining ($r=0.03$, $F=.046$, $p=.8386$; Figure 5d).

NHERF1 interferes with Fzd-Dvl binding

Due to the short C-terminal tail of Fzd receptors, the Dvl and NHERF1 binding sites are separated by as few as 13 amino acids. Therefore, we hypothesized that interaction between NHERF1 and Fzd may alter the recruitment and activation of Dvl. To investigate this we co-immunoprecipitated HA-Fzd4 and myc-Dvl2 in the presence or absence of NHERF1. In the absence of NHERF1, Fzd4 co-immunoprecipitated notably greater amounts of Dvl2 (Figure 6a, compare lane 1 and 2). After stimulation with Wnt, identical amounts of Dvl were co-immunoprecipitated suggesting that Wnt binding induces dissociation of NHERF1 and binding to Dvl (Figure 6a, lanes 3 and 4). To confirm that this was the case, the effects of

Wnt-conditioned medium on the co-immunoprecipitation of HA-Fzd4 and NHERF1 was examined using CHO-N10 cells. The results demonstrate that Wnt induces dissociation of NHERF1 and Fzd4 (Supplementary Figure 3).

Total internal reflection fluorescence (TIRF) microscopy was used to investigate the effects of NHERF1 on Fzd-Dvl interactions with greater temporal resolution. TIRF allows imaging of a very thin optical section containing the plasma membrane, such that changes in the fluorescence intensity detected by TIRF reflect traffic of the fluorescent protein to and from the plasma membrane. mRed-Dvl2 was found to be uniformly distributed in the cytoplasm in CHO-N10 cells expressing NHERF1 (Figure 6b). Upon stimulation with Wnt5a, Dvl2 was recruited to the membrane (Figure 6d). In control cells, Dvl2 was localized to the plasma membrane under basal conditions (Figure 6c). The addition of Wnt had no effect on the amount of Dvl2 at the plasma membrane (Figure 6d). These data suggest that Wnt binding causes a slow dissociation of NHERF1 resulting in a retardation of the coupling of Fzd and Dvl. These observations imply, therefore, that the effects of NHERF1 on Wnt signaling are a consequence of the inhibition of Fzd-Dvl pre-coupling, which results in slower, significantly attenuated responses.

Coupling between Fzd receptors and Dvl has been shown to be critical for proper Fzd internalization and signaling (Chen et al., 2003; Yu et al., 2007). Thus, the binding of NHERF1 to Fzd should reduce Fzd-Dvl pre-coupling and result in impaired Wnt-induced Fzd internalization. Consistent with this hypothesis, CHO-N10 cells lacking NHERF1 internalized a remarkable 70% of their Fzd4 receptors in response to Wnt5a, whereas less than 20% of the surface Fzd4 is internalized in cells expressing NHERF1 (Figure 6e). In contrast, the endocytosis of the V537A-Fzd4 mutant is insensitive to the expression of NHERF1, internalizing readily whether NHERF1 is expressed or not (Figure 6e).

Based on the results presented here, we propose the following model for the regulatory role of NHERF1 in breast cancer (Figure 6f). Normal breast tissues and low grade ductal carcinomas express NHERF1, which attenuates Wnt signaling by impairing Fzd-Dvl pre-coupling. Under these conditions, the growth of breast epithelia is mainly controlled by estrogen-regulated signals. As the tumor progresses NHERF1 expression diminishes due to genetic changes or as a consequence of treatment with anti-estrogens. Reduced levels of NHERF1 facilitate coupling of Fzd receptors to Dvl and, subsequently, enhanced Wnt signaling. Wnt then becomes a driving force in the proliferation of the tumor, inducing epithelial-mesenchymal transition and resulting in increasing malignancy and tumor metastasis.

DISCUSSION

Our findings show that NHERF1 regulates canonical Wnt signaling. We demonstrate that NHERF1 modulates Dvl recruitment and Wnt-induced β-catenin activation through direct interactions between the second PDZ domain of NHERF1 and the C-terminal PDZ ligand of a selected subset of Fzd receptors. In the absence of NHERF1, Fzd precouples with Dvl resulting in augmented canonical Wnt signaling. This conclusion is further supported by the finding that NHERF1 knockout mice display increased mammary duct proliferation and

density correlated with increased β-catenin activation. Likewise, human breast tumors show a significant negative correlation between NHERF1 expression and β-catenin activation. We conclude, therefore, that NHERF1 expression is required for proper Wnt signaling in normal mammary epithelium. Loss of NHERF1 results in dysregulation of Wnt function that leads to increased proliferation and possibly dysplastic changes of the mammary epithelium. Whether this is NHERF1's main role in the regulation of mammary tissues remains to be determined. A recent report has linked NHERF1 to the regulation of the tumor suppressor PTEN and the subsequent attenuation of PDGF signaling in breast cancer (Pan et al., 2008). Thus, in mammary epithelium, NHERF1 appears to have multiple functions that converge in the regulation of normal cell proliferation.

Our findings show that NHERF1 inhibits Fzd2, Fzd4 and Fzd7 but not Fzd3-dependent β-catenin activation. Thus, Wnt signaling is expected to be insensitive to NHERF1 expression in cells harboring high levels of Fzd3. Likewise, because Fzd6 does not contain a canonical PDZ ligand sequence in its C-terminus, we predict that Fzd6 signaling will be insensitive to NHERF1 expression. Thus, since only a subset of Fzd receptors are targets for NHERF1 regulation, the expression profile of the Fzd receptors in breast tumors is of primary interest. Importantly, the Fzd expression profile of breast cancer cells shows a predominance of Fzd5, Fzd2 and Fzd1, which account for well over 90% of the Fzd mRNA produced by MCF7 cells (Supplementary Table 1) and contain canonical PDZ ligand sequences. A similar expression profile was found in MDA MB-231 cells, suggesting that this pattern of expression may be typical for breast epithelium. Furthermore, our data demonstrate that Wnt signaling is attenuated by NHERF1 expression in both MCF7 and MDA-MB231 cells, confirming the hypothesis that NHERF1 regulates Wnt signaling in breast cancer.

Normal and malignant breast tissues express several other PDZ proteins that reportedly interact with Fzd receptors. For instance, syntenin, an adaptor protein that, like NHERF1, contains 2 PDZ domains in tandem, reportedly interacts with a subset of Fzd receptors and modulates non-canonical Wnt signaling during the embryonic development of *Xenopus* (Luyten et al., 2008). Furthermore, syntenin is highly expressed in breast cancer tissues, also mediating non-canonical Wnt signaling and inducing cell migration and invasion (Koo et al., 2002). However, there is no evidence that syntenin regulates canonical Wnt signaling in any way. In fact, neither the knockdown nor the overexpression of syntenin have any effects on the activation of the β-catenin pathway during *Xenopus* development (Luyten et al., 2008).

A second PDZ protein expressed in epithelial tissues is the membrane-associated guanylate kinase family member MAGI-3 (Laura et al., 2002). MAGI-3 contains six PDZ domains in tandem, and reportedly interacts with Fzd4 via its second PDZ domain (Yao et al., 2004). This interaction modulates the activation of Jnk and the non-canonical Wnt signaling pathway. However, as in the case of syntenin, the interactions of MAGI-3 and Fzd receptors do not affect β-catenin signaling in any measurable way (Yao et al., 2004). Associations between Fzd receptors and several other PDZ proteins have been reported in mammalian systems (Wawrzak et al., 2009). However, most reported interactions have been linked exclusively to the positive modulation of non-canonical Wnt signaling. In general, no evidence of the regulation of Wnt-dependent β-catenin activation by PDZ proteins has been

reported to date in mammalian systems. NHERF1 is, therefore, unique among PDZ proteins in its role as a negative regulator of Wnt-dependent β-catenin signaling in breast epithelium.

Some recent reports have suggested that NHERF1 is overexpressed in breast cancer cells as compared to normal mammary tissues (Cardone et al., 2007; Mangia et al., 2009; Song et al., 2007). Although this is not surprising because NHERF1 expression is positively regulated by the estrogen receptor (Ediger et al., 1999), it implies that loss of NHERF1 is unlikely to be the primary cause of the transformed phenotype. However, NHERF1 expression is greatly reduced in the more invasive ER-negative tumors (Song et al., 2007; Stemmer-Rachamimov et al., 2001). These findings suggest a unique role for NHERF1 in the evolution of estrogen driven ER-positive tumors into more aggressive Wnt driven tumors. In ER-positive ductal carcinomas, which express NHERF1, proliferation is driven by classical ER-dependent pathways with relatively little contribution from Wnt signaling. We propose that loss of NHERF1 via genetic or epigenetic changes increases the contribution of Wnt signaling in tumor growth, thus allowing the loss of the ER, promoting epithelial-to-mesenchymal (EMT) transition and increasing tumor aggressiveness.

If true, this hypothesis may have significant implications for the treatment of ER-positive breast cancer. The majority of ER-positive carcinomas are successfully treated with anti-estrogens, such as tamoxifen, which inhibit ER-dependent growth. However, tamoxifen treatment reduces NHERF1 expression by approximately 70% in cell culture systems (Ediger et al., 1999). Chronic treatment with anti-estrogens will likely decrease NHERF1 expression in the tumor, which would increase its sensitivity to Wnt ligands, thus switching the proliferative drive from estrogen dependent to Wnt dependent. This model explains the paradoxical observation that ER-positive tumors recurring after prolonged anti-estrogen treatment are inhibited by the administration of estrogens (Ellis et al., 2009). We propose that this inhibition is mediated by estrogen-induced expression of NHERF1, which then inhibits Wnt-dependent proliferation. This model highlights the importance of NHERF1 as a marker for Wnt sensitivity and the importance of targeting the Wnt signaling pathways for the treatment of breast carcinomas.

Methods

Breast biopsies

All biopsy samples were obtained in accordance with the University of Pittsburgh Internal Review Board. Sample characteristics are summarized in Supplementary Table 2.

Materials and constructs

Anti-NHERF1, anti-β-catenin, anti-myc and anti-HA (HA.11) antibodies were purchased from Upstate Biotechnology, Millipore, Sigma, and Covance. Secondary antibodies were from Jackson ImmunoResearch. TRITC conjugated phalloidin was purchased from Invitrogen. All other materials were purchased from Sigma unless otherwise indicated. Human Fzd 2, 3, and 7 were purchased from OpenBiosystems, Inc. and subcloned into pcDNA3.1(+) using EcoRI and XhoI. NHERF1-targeted shRNA plasmids have been previously described (Wang et al., 2007). TOP and FOP plasmids were supplied by Dr. Paul

Monga. Fzd4-HA, Fzd4-eGFP, myc-Dvl2 and mRed-Dvl2 plasmids were kindly provided by Dr. T. Kirchhausen (Yu et al., 2007).

Cell culture

CHO-N10 cells were grown as described (Wheeler et al., 2007). MCF7 and MDA MB-231 cells were grown in DMEM/F12 medium (Mediatech, Inc.) supplemented with 10% fetal bovine serum (Invitrogen) and 1% penicillin/streptomycin. Wnt-3a, Wnt-5a and control L-cells were purchased from ATCC and grown in DMEM supplemented with 10% fetal bovine serum and 1% penicillin/streptomycin. Conditioned media was removed from cells after four days in culture and returned to a pH of 7.4 by addition of HEPES buffer. FuGENE 6 (Roche Applied Sciences) was used for all transfections.

Fluorescence Recovery After Photobleaching (FRAP)

FRAP was conducted as described previously (Wheeler et al., 2007). Briefly, cells seeded onto Mattek dishes were transfected with the indicated plasmids. Small circular regions of the plasma membrane were bleached with a 405nm laser line and images were collected every second for 1–2 minutes. The images were exported to ImageJ (NIH) and the average fluorescent intensity of the bleached region was measured. The diffusion coefficient was calculated using the Stokes-Einstein equation for two-dimensional diffusion. The bar graph represents aggregate data from approximately 20 cells imaged over three sessions.

Total Internal Reflection Fluorescence (TIRF) Microscopy

TIRF studies were done as previously described (Wheeler et al., 2007). Red and green TIRF images were collected sequentially every 5 seconds for 15 minutes. A baseline was established with 2 minutes of imaging prior to the addition of Wnt5a. The average Dvl2 intensity was normalized to the average Fzd intensity and graphed using GraphPad Prism.

Receptor Internalization

Internalization of membrane proteins was measured using flow cytomerty as described (Garrido et al., 2009). CHO-N10 cells stably transfected with HA-Fzd4 containing an extracellular HA epitope were treated with Wnt5a, washed twice with ice-cold PBS and fixed with 0.5% paraformaldehyde for 5 minutes. This protocol left the cell membrane intact and impermeant to antibodies. Cells were scraped and incubated in 3% bovine serum albumin for 30 minutes to block non-specific binding. The cells were stained with anti-HA (Covance) followed by anti-rabbit-Alexa-680. The fluorescence of each cell was measured using a flow cytometer and reflected the amount of Fzd4 on the surface. Percentage Fzd internalization was calculated as: $100 \times (1 - \text{geometric mean fluorescence (t)} / \text{geometric mean fluorescence (t=0)})$.

Quantitative breast histology

The fourth and fifth breasts of 10 week old NHERF1+/+ and NHERF1−/− mice were removed and fixed in buffered formalin. Following fixation, they were embedded in paraffin and sectioned. Slides from different depth in the breast tissue were stained with haematoxylin and eosin. Each slide was imaged 10 times at 20× magnification. Coordinates

were randomly generated; if breast tissue did not occupy 90% of the visual field, new coordinates were generated. The average number of ducts per field was calculated for each slide. The bar chart represent average ducts per field measured from 3 NHERF1 +/+ animals and 5 NHERF1 −/− animals (2 having the more severe phenotype). For BrdU staining the animals were injected with 50 μg/g of body weight 6 h before harvesting the breast tissues. BrdU incorporation was determined with anti-BrdU antibody (GE Healthcare).

TOP/FOP Luciferase assay

Cells were stimulated with control, Wnt3a-, or Wnt5a-enriched medium for 8 hours. Cells were lysed with Reporter Lysis Buffer (Promega) and transferred to a 96-well plate. The luminescence of each well was recorded for 5 seconds after addition of BioGlo Luciferase substrate (Promega). The ratio of TOP/FOP signal was calculated and normalized to control conditions. Bars represent data from at least three experiments conducted in duplicate.

Quantitative Real-Time PCR (qPCR)

RNA was extracted using Trizol (Invitrogen) and transcribed into cDNA using a Clontech Advantage RT-for-PCR kit. Quantitative real-time PCR was performed on an Applied BioSystems StepONe real-time PCR system using SYBR Green (Qiagen) with the primers listed in Supplementary Table 3. All samples were run in duplicate and normalized to GAPDH.

Statistical Analysis

Each experiment was repeated at least three times. All statistical tests were conducted using GraphPad Prism.

Supplementary Material

Refer to Web version on PubMed Central for supplementary material.

ACKNOWLEDGEMENTS

This work was supported by grants DK083211 (DSW), DK079864 (GR) and DK54171 (PAF) from the National Institutes of Health. We also acknowledge support from the Office of the Senior Vice Chancellor for the Health Sciences of the University of Pittsburgh (GR).

References

Ayyanan A, Civenni G, Ciarloni L, Morel C, Mueller N, Lefort K, Mandinova A, Raffoul W, Fiche M, Dotto GP, Brisken C. Proc Natl Acad Sci U S A. 2006; 103:3799–3804. [PubMed: 16501043]

Bates IR, Hebert B, Luo Y, Liao J, Bachir AI, Kolin DL, Wiseman PW, Hanrahan JW. Biophys J. 2006; 91:1046–1058. [PubMed: 16714353]

Cardone RA, Bellizzi A, Busco G, Weinman EJ, Dell'Aquila ME, Casavola V, Azzariti A, Mangia A, Paradiso A, Reshkin SJ. Mol Biol Cell. 2007; 18:1768–1780. [PubMed: 17332506]

Chen W, ten Berge D, Brown J, Ahn S, Hu LA, Miller WE, Caron MG, Barak LS, Nusse R, Lefkowitz RJ. Science. 2003; 301:1391–1394. [PubMed: 12958364]

Dai JL, Wang L, Sahin AA, Broemeling LD, Schutte M, Pan Y. Oncogene. 2004; 23:8681–8687. [PubMed: 15467753]

Dolled-Filhart M, McCabe A, Giltnane J, Cregger M, Camp RL, Rimm DL. Cancer Res. 2006; 66:5487–5494. [PubMed: 16707478]

Ediger TR, Kraus WL, Weinman EJ, Katzenellenbogen BS. Endocrinology. 1999; 140:2976–2982. [PubMed: 10385389]

Ellis MJ, Gao F, Dehdashti F, Jeffe DB, Marcom PK, Carey LA, Dickler MN, Silverman P, Fleming GF, Kommareddy A, Jamalabadi-Majidi S, Crowder R, Siegel BA. JAMA. 2009; 302:774–780. [PubMed: 19690310]

Fantozzi A, Christofori G. Breast Cancer Res. 2006; 8:212. [PubMed: 16887003]

Garrido JL, Wheeler D, Vega LL, Friedman PA, Romero G. Mol Endocrinol. 2009; 23:2048–2059. [PubMed: 19837945]

Gillett C, Smith P, Gregory W, Richards M, Millis R, Peters G, Barnes D. Int J Cancer. 1996; 69:92–99. [PubMed: 8608989]

Karthikeyan S, Leung T, Birrane G, Webster G, Ladias JA. J Mol Biol. 2001; 308:963–973. [PubMed: 11352585]

Koo TH, Lee JJ, Kim EM, Kim KW, Kim HD, Lee JH. Oncogene. 2002; 21:4080–4088. [PubMed: 12037664]

Kreimann EL, Morales FC, de Orbeta-Cruz J, Takahashi Y, Adams H, Liu TJ, McCrea PD, Georgescu MM. Oncogene. 2007; 26:5290–5299. [PubMed: 17325659]

Laura RP, Ross S, Koeppen H, Lasky LA. Exp Cell Res. 2002; 275:155–170. [PubMed: 11969287]

Lin SY, Xia W, Wang JC, Kwong KY, Spohn B, Wen Y, Pestell RG, Hung MC. Proc Natl Acad Sci U S A. 2000; 97:4262–4266. [PubMed: 10759547]

Luyten A, Mortier E, Van Campenhout C, Taelman V, Degeest G, Wuytens G, Lambaerts K, David G, Bellefroid EJ, Zimmermann P. Mol Biol Cell. 2008; 19:1594–1604. [PubMed: 18256285]

Mangia A, Chiriatti A, Bellizzi A, Malfettone A, Stea B, Zito FA, Reshkin SJ, Simone G, Paradiso A. Histopathology. 2009; 55:600–608. [PubMed: 19912366]

Pan Y, Wang L, Dai JL. Breast Cancer Res. 2006; 8:R63. [PubMed: 17078868]

Pan Y, Weinman EJ, Dai JL. Breast Cancer Res. 2008; 10:R5. [PubMed: 18190691]

Ryo A, Nakamura M, Wulf G, Liou YC, Lu KP. Nat Cell Biol. 2001; 3:793–801. [PubMed: 11533658]

Song J, Bai J, Yang W, Gabrielson EW, Chan DW, Zhang Z. Histopathology. 2007; 51:40–53. [PubMed: 17593079]

Songyang Z, Fanning AS, Fu C, Xu J, Marfatia SM, Chishti AH, Crompton A, Chan AC, Anderson JM, Cantley LC. Science. 1997; 275:73–77. [PubMed: 8974395]

Stemmer-Rachamimov AO, Wiederhold T, Nielsen GP, James M, Pinney-Michalowski D, Roy JE, Cohen WA, Ramesh V, Louis DN. Am J Pathol. 2001; 158:57–62. [PubMed: 11141479]

Tetsu O, McCormick F. Nature. 1999; 398:422–426. [PubMed: 10201372]

Umekita Y, Ohi Y, Sagara Y, Yoshida H. Int J Cancer. 2002; 98:415–418. [PubMed: 11920593]

Wang B, Bisello A, Yang Y, Romero GG, Friedman PA. J Biol Chem. 2007; 282:36214–36222. [PubMed: 17884816]

Wawrzak D, Luyten A, Lambaerts K, Zimmermann P. Adv Enzyme Regul. 2009; 49:98–106. [PubMed: 19534027]

Weinman EJ, Hall RA, Friedman PA, Liu-Chen LY, Shenolikar S. Annu Rev Physiol. 2006; 68:491–505. [PubMed: 16460281]

Wheeler D, Sneddon WB, Wang B, Friedman PA, Romero G. J Biol Chem. 2007; 282:25076–25087. [PubMed: 17599914]

Yao R, Natsume Y, Noda T. Oncogene. 2004; 23:6023–6030. [PubMed: 15195140]

Yu A, Rual JF, Tamai K, Harada Y, Vidal M, He X, Kirchhausen T. Dev Cell. 2007; 12:129–141. [PubMed: 17199046]

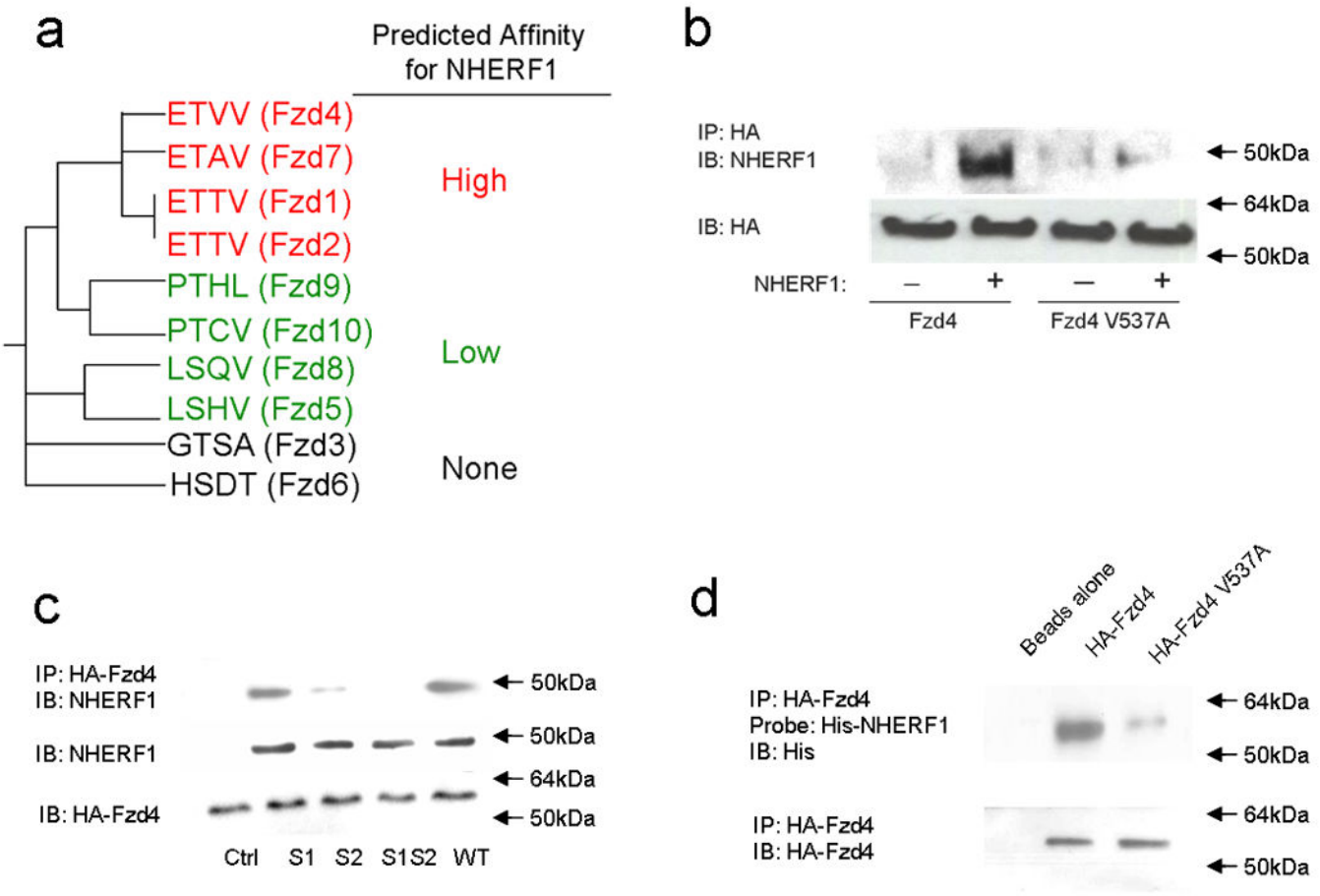

Figure 1. NHERF1 interacts with the C-terminal PDZ ligand of Frizzled receptors

(**a**) Human Fzd receptors cluster into three groups based on alignment of their C-termini. Fzd 1, 2, 4 and 7 terminate in the consensus sequence E-T-x-V which is predicted to have high affinity for the PDZ domains of NHERF1 (Karthikeyan et al., 2001). The C-terminal sequences of Fzd 5, 8, 9 and 10 are also expected to bind PDZ domains but are predicted to have lower affinity for NHERF1. Fzd 3 and 6 do not terminate in a consensus PDZ ligand and thus are not expected to interact with NHERF1. (**b**) NHERF1 co-immunoprecipitates with HA-Fzd4 in CHO-N10 cells. Mutation of the C-terminal valine to alanine (V537A) abrogates this interaction. (**c**) Fzd4 interacts primarily with the second PDZ domain of NHERF1 (PDZ2). CHO cells were transfected with NHERF1 mutants (S1: mutated PDZ1, S2: mutated PDZ2; S1S2: mutated in both PDZ domains; WT: wild type). (**d**) The binding of NHERF1 to Fzd4 is caused by direct interactions. HA-tagged Fzd4 was expressed in CHO cells, extracted and incubated with specific agarose beads linked to anti-HA antibody or with beads in the absence of anti-HA antibody. The material bound to the beads was resolved by SDS-PAGE and blotted onto nitrocellulose. The blot was developed with recombinant His-tagged NHERF1 isolated from *E. coli* followed by HRP-tagged anti-His antibody. The only NHERF1-positive bands present in the gel corresponded to the molecular weight of the immunoprecipitated HA-Fzd4.

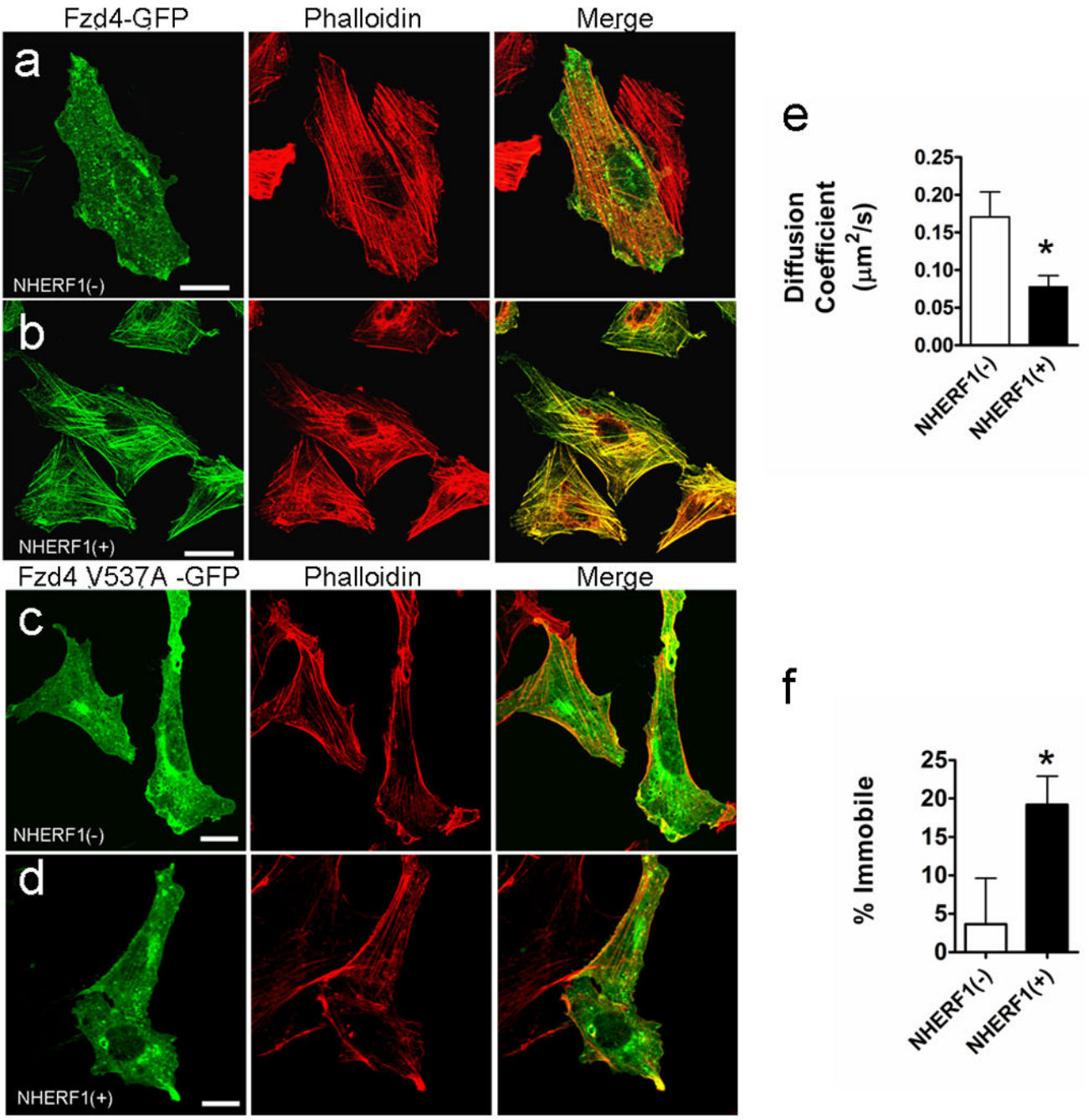

Figure 2. NHERF1 modulates the distribution and dynamics of Fzd4

(**a**) CHO-N10 cells were transiently transfected with Fzd4-eGFP and stained with TRITC conjugated phalloidin. Fzd4-eGFP has a uniform membrane distribution and does not co-localize with phalloidin-stained actin fibers. (**b**) Expression of NHERF1 causes Fzd4-eGFP to aggregate along phalloidin-positive actin fibers. (**c–d**) Expression of NHERF1 does not alter membrane distribution of Fzd4 V537A-eGFP consistently with the inability of this mutant to bind PDZ domains. Scale bar represents 5 μm. (**e–f**) The lateral mobility of Fzd-eGFP in control and NHERF1 expressing CHO-N10 cells was measured by FRAP.

NHERF1 expression decreased the diffusion coefficient of Fzd4-eGFP from 0.17 $\mu m^2/s$ to 0.07 $\mu m^2/s$. NHERF1 expression also caused a concomitant 5 fold increase in the immobile fraction (* $p < 0.05$, Students' T-test).

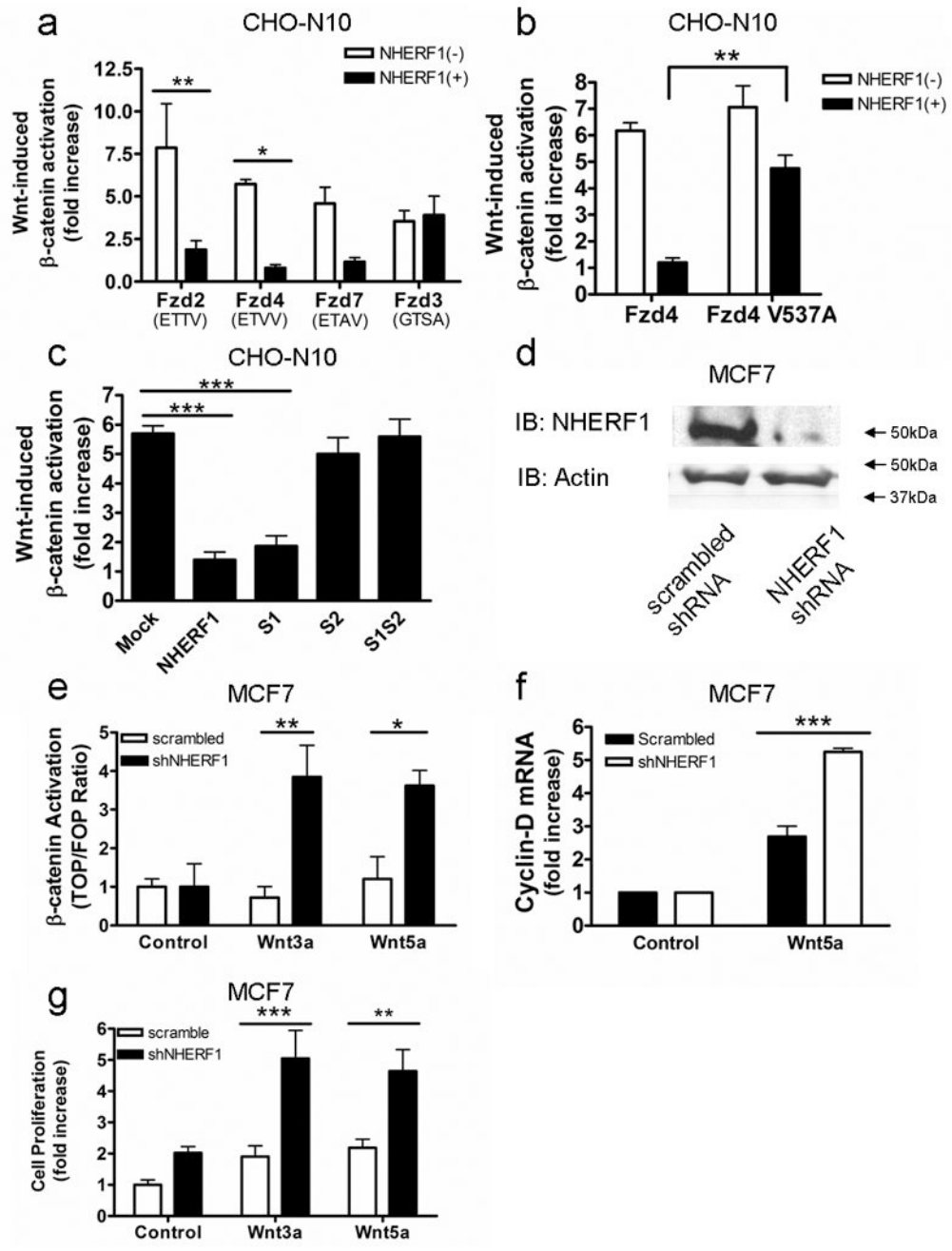

Figure 3. Enhanced Wnt signaling occurs in the absence of NHERF1

(**a**) CHO-N10 cells were co-transfected with the indicated Fzd receptors and either TOP or FOP luciferase reporter plasmid. NHERF1 expression blunted Wnt-induced luciferase expression via Fzd 2, 4 and 7 but had no effect on Wnt signaling through Fzd3 (** $p < 0.01$, * $p < 0.05$, Two-way ANOVA with Bonferroni post-hoc tests). (**b**) Mutational ablation of the Fzd4 PDZ ligand (Fzd4 V573A) rescues Wnt signaling from NHERF1 inhibition. This mutation has no effect on Wnt singaling in the absence of NHERF1. (**c**) Wnt-induced β-catenin activation was blocked by wild type NHERF1 and NHERF1 containing a mutated

PDZ1 domain (S1). This inhibition was not caused by expression of NHERF1 containing a mutated PDZ2 domain (S2) or with both PDZ domains mutated (S1S2) (*** $p < 0.001$, One-way ANOVA with Tukey post-hoc tests). (**d**) Transfection of MCF7 cells with NHERF1 targeted shRNA reduced expression by 95%. (**e**) NHERF1 knockdown enhanced Wnt-induced β-catenin activation in MCF7 cells (* $p < 0.05$, ** $p < 0.01$, Two-way ANOVA with Bonferroni post-hoc tests). (**f**) Following 8-hours of treatmnent with Wnt, NHERF1 knockdown cells shown increased levels of cyclin-D1. (*** $p < 0.001$, Two-way ANOVA with Bonferroni post-hoc tests). (**g**) Wnt-induced proliferation was measured using a 24 hours radiolabeled-thymidine incorporation assay. MCF7 cells lacking NHERF1 showed marked proliferative responses to both Wnt3a and Wnt5a compared to scrambled controls (** $p < 0.01$, *** $p < 0.001$, Two-way ANOVA with Bonferroni post-hoc tests).

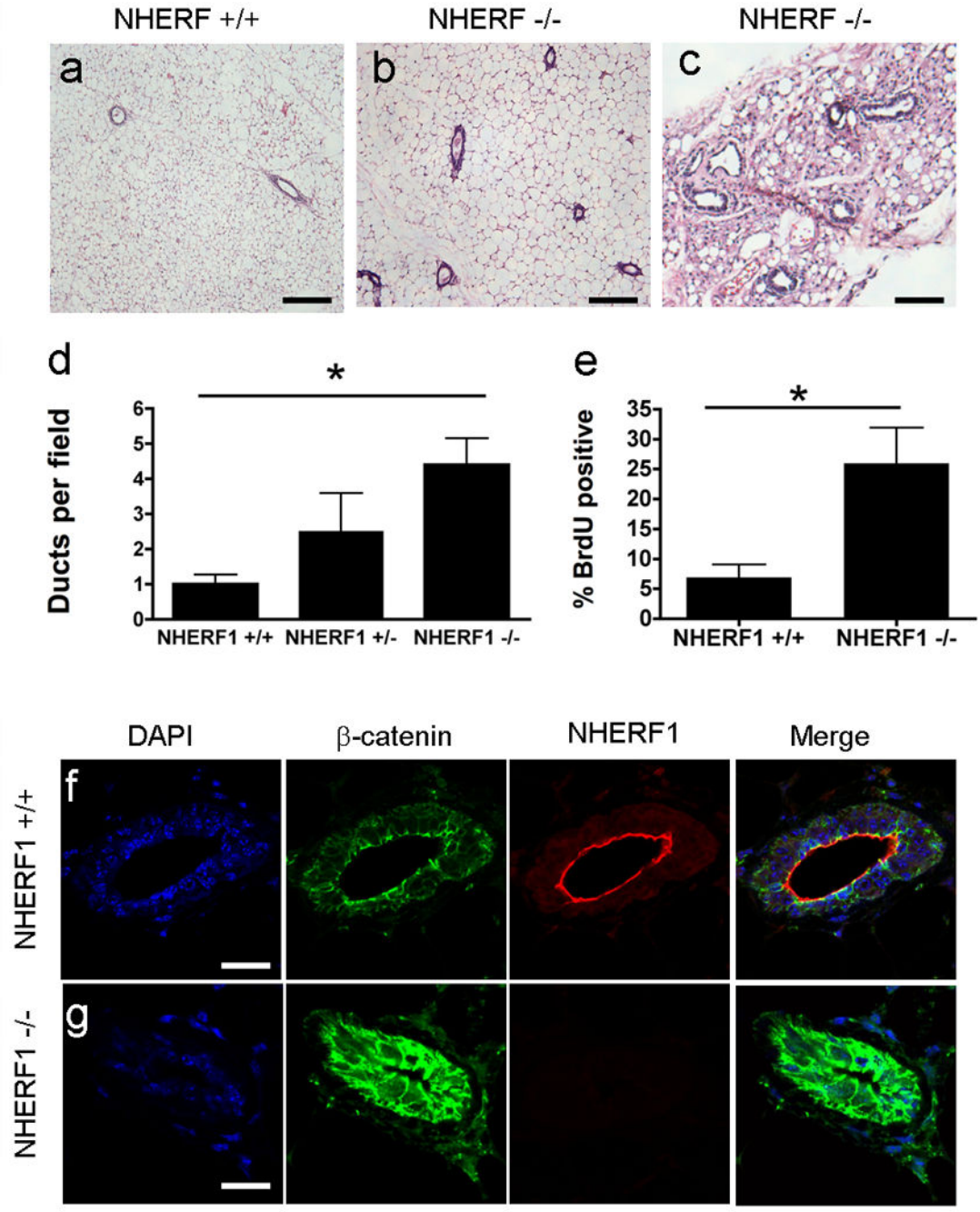

Figure 4. Mammary glands of NHERF1 knock-out mice exhibit increased β-catenin signaling, elevated ductal density, and increased cell proliferation

The fourth and fifth breasts from virgin NHERF1+/+ and NHERF1−/− littermates were removed and histologically prepared. (**a**) Representative images from 10 week old NHERF1+/+ mouse. (**b**) Representative images from a 10 week old NHERF1−/− mouse. (**c**) A subset of NHERF1−/− mice presented a more severe phenotype characterized by a loss of adipose tissue, capillary dilation and ductal dilation. Scale bar represents 200 μm. (**d**) Quantification of ductal density in NHERF1+/+ and NHERF1−/− mice (* $p < 0.05$,

Students' T test). (**e**) Increased mammary duct proliferation in NHERF1−/− females. (**f**) Individual duct from NHERF1+/+ mouse stained with DAPI (blue), anti-β-catenin (green) and anti-NHERF1 (red). NHERF1 decorates the apical surface while β-catenin staining is observed along all membranes of the epithelial cells. Scale bar represents 20 μm. (**f**) Individual duct from NHERF1−/− mouse. β-catenin staining is augmented and is no longer restricted to the membrane. Scale bar represents 20 μm.

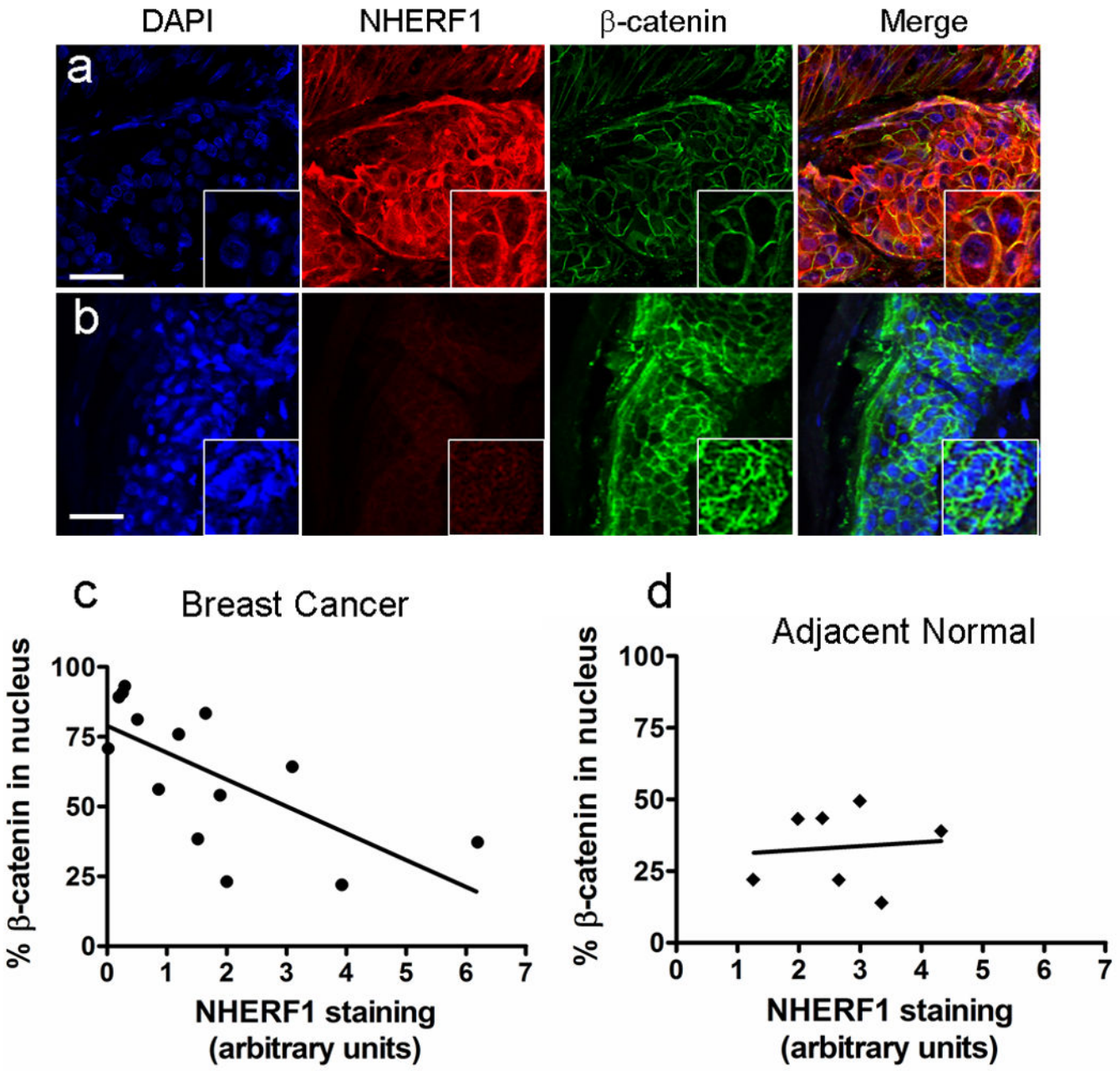

Figure 5. β-catenin activation and NHERF1 expression are negatively correlated in human breast cancer samples

Human breast cancer biopsies were stained with DAPI (blue), anti-β-catenin (green) and anti-NHERF1 (red). (*a*) Samples which robustly expressed NHERF1 had a faint, membranous β-catenin staining pattern. There was minimal colocalization between β-catenin staining and nuclear DAPI staining (insert). (*b*) Samples with nominal NHERF1 staining exhibited a large percentage of β-catenin staining within the nucleus. Scale bar represents 20 μm in the main panel and 10 μm in insert. (**c**) NHERF1 expression is negatively correlated

with the percentage of β-catenin staining occurring within the nucleus. (**d**) No correlation between NHERF1 expression and nuclear β-catenin is observed in adjacent normal tissue.

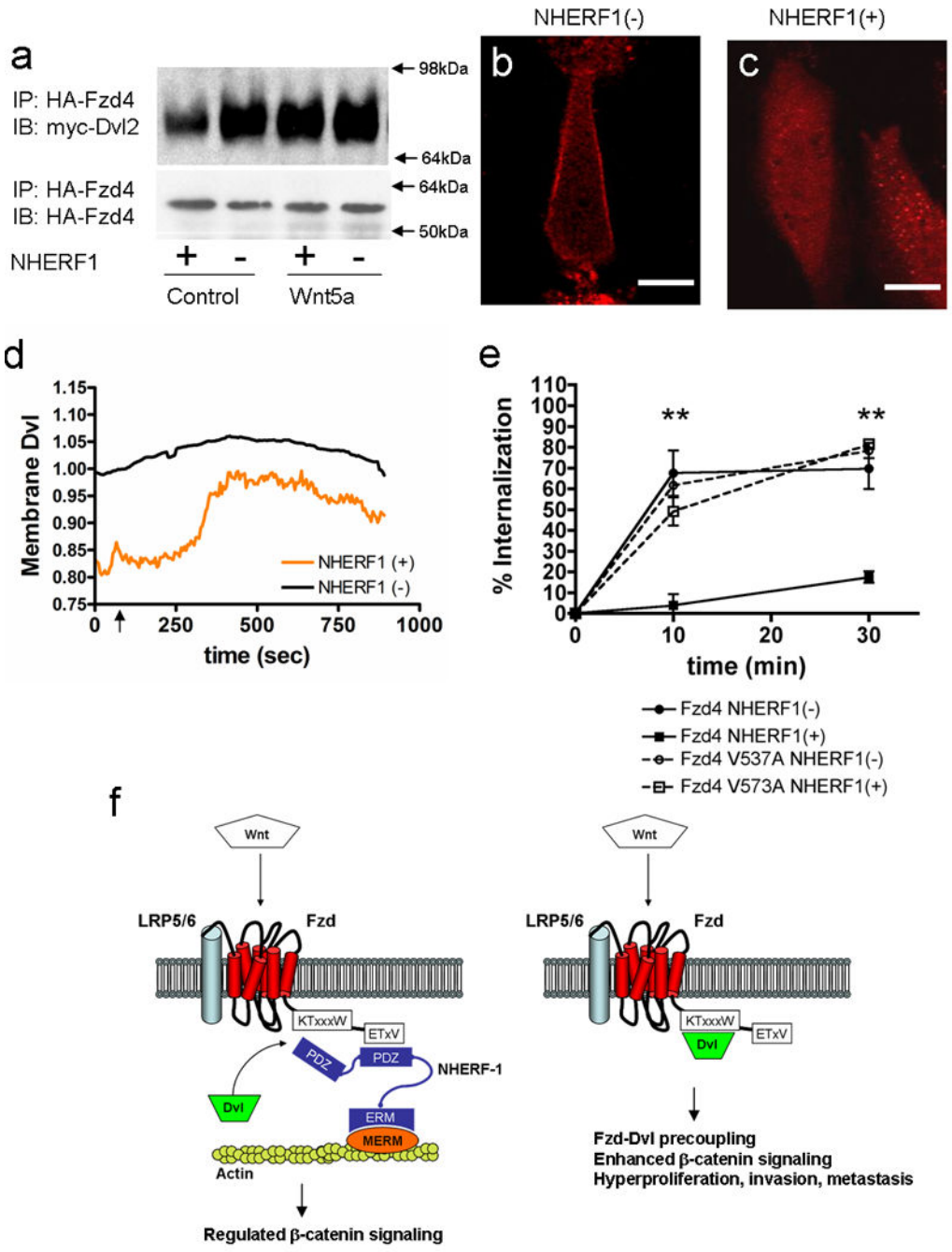

Figure 6. Fzd-Dvl precoupling is disrupted by NHERF1

(**a**) Co-immunoprecipitation between myc-Dvl2 with HA-Fzd4 was assessed in CHO-N10 cells before and 10 minutes following Wnt5a treatment. Interaction between Dvl2 and Fzd was clearly enhanced in the absence of NHERF1 prior to Wnt5a addition. The amount of Dvl2-Fzd complex following treatment with Wnt5a was independent of NHERF1 expression. (**b**) mRed-Dvl2 has a uniform cytoplasmic distribution in CHO-N10 cells expressing Fzd4 and NHERF1. (**c**) In the absence of NHERF1, mRed-Dvl2 localizes predominantly to the membrane. Scale bar represents 5 μm. (**d**) CHO-N10 cells expressing

mRed-Dvl2 and Fzd4-GFP were rapidly imaged using TIRF microscopy. All intensity measurements are normalized to Fzd4-GFP to account for receptor internalization. Addition of Wnt5a is indicated by an arrow. In NHERF1 expressing cells, the addition of Wnt5a induced a translocation of Dvl2 to the plasma membrane. The amount of membrane associated Dvl2 did not change with addition of Wnt5a in control cells. (**e**) Fzd4 internalization was inferred from decreases in surface staining as measured by flow cytometry. In the absence of NHERF1, Wnt5a trigger extensive Fzd4 internalization (** $p = 0.002$, Student's T-test). As expected, the internalization of the V537A-Fzd4 mutant is insensitive to NHERF1 expression. (**f**) In normal mammary epithelium, NHERF1 occupies the C-terminus of Fzd receptors tethering it to the actin cytoskeleton. Loss of NHERF1 allows abnormal Fzd-Dvl precoupling which results in pathologically enhanced Wnt-induced β-catenin activation and hyper-proliferation.